

# Enhanced Luminescent Properties of an Open-Shell (3,5-Dichloro-4-pyridyl)bis(2,4,6-trichlorophenyl)methyl Radical by Coordination to Gold\*\*

Yohei Hattori, Tetsuro Kusamoto,\* and Hiroshi Nishihara\*

**Abstract:** A gold(I) complex containing an open-shell luminescent (3,5-dichloro-4-pyridyl)bis(2,4,6-trichlorophenyl)methyl (PyBTM) radical was prepared. The complex showed fluorescence centered mainly on the coordinated PyBTM ligand. The photophysical and photochemical properties were positively modulated upon coordination to Au<sup>I</sup>; the photoluminescence quantum yield, fluorescence wavelength, and the stability in the photoexcited state all increased.

Spin multiplicity is an important issue in fundamental and applied research of luminescent molecules. In closed-shell luminescent molecules, fluorescence from singlet excited states (S<sub>1</sub>) and phosphorescence from the triplet excited state (T<sub>1</sub>) have been extensively studied. The introduction of open-shell radical species into luminescent closed-shell molecules often quenches their fluorescence. In paramagnetic Cu<sup>II</sup>-porphyrin<sup>[1]</sup> and Zn-porphyrin with a coordinated nitronyl nitroxide radical,<sup>[2]</sup> fluorescence from singlet excited states of the porphyrin (<sup>2</sup>S<sub>1</sub>=D<sub>2</sub>) are quenched via quartet (<sup>4</sup>T<sub>1</sub>=Q<sub>1</sub>) and doublet (<sup>2</sup>T<sub>1</sub>=D<sub>1</sub>) states at a lower energy derived from the triplet excited state of the porphyrin. Spin-labeled luminogens act as fluorescent probes; the luminescent off state of the probes is switched to the on state by the loss of its radical character upon the reaction with other radical species such as •OH.<sup>[3]</sup> Recently, the luminescence of open-shell organic molecules, such as doublet monoradicals, has attracted much interest owing to the characteristic photofunctions.<sup>[4]</sup> These radicals show fluorescence from the lowest excited doublet state (D<sub>1</sub>) to the ground doublet state (D<sub>0</sub>).

We have recently reported the fluorescence of a novel organic radical, (3,5-dichloro-4-pyridyl)bis(2,4,6-trichlorophenyl)methyl radical (PyBTM), which is stable under

ambient condition and photoirradiation.<sup>[5]</sup> The nitrogen atom of PyBTM, which enhances its photostability (up to 115 times higher than tris(2,4,6-trichlorophenyl)methyl radical), acts as a proton coordination site. The electronic and optical properties were controlled by reversible protonation; the fluorescence intensity decreased largely upon protonation. Thanks to its stimuli-responsive properties and high photostability, PyBTM is a promising candidate for investigating the characteristic luminescent properties of doublet species controlled by external stimuli.

Our next aim is to enhance the luminescent properties of PyBTM through its coordination to metal. Although the fluorescence properties of perchlorinated triphenylmethyl radicals have been modulated by chemical modification with organic moieties,<sup>[4]</sup> to our knowledge there are no examples of using coordination chemistry to prepare luminescent open-shell species with unique photofunctions. This aim is challenging because the luminescence of a radical ligand is usually quenched by coordination to a metal; for example, a carboxylate ligand with luminescent radicals loses its luminescent properties upon coordination to metal ions.<sup>[6]</sup>

Herein we report the synthesis of a Au<sup>I</sup> complex with PyBTM as a ligand, [Au<sup>I</sup>(PyBTM)PPh<sub>3</sub>]<sup>+</sup>X<sup>-</sup> (1X; X = ClO<sub>4</sub><sup>-</sup>, BF<sub>4</sub><sup>-</sup>; Figure 1), and its photophysical and photochemical

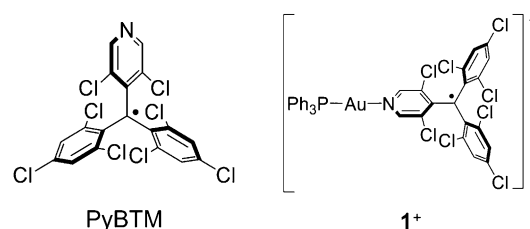


Figure 1. Structure of PyBTM and 1<sup>+</sup>.

properties. We chose Au<sup>I</sup> as a metal center because it can form a strong coordination bond with pyridine derivatives, and gold complexes often show superior luminescence properties.<sup>[7]</sup>

[Au<sup>I</sup>(PyBTM)PPh<sub>3</sub>]<sup>+</sup>ClO<sub>4</sub><sup>-</sup> (1ClO<sub>4</sub>) was synthesized from [Au<sup>I</sup>(PPh<sub>3</sub>)Cl] and PyBTM by using AgClO<sub>4</sub> to remove a chloro ligand as an AgCl precipitate.<sup>[8]</sup> The complex was characterized by ESI-TOF-MS and elemental analysis. 1ClO<sub>4</sub> was used for single-crystal X-ray diffraction, ESR measurement, and cyclic voltammetry. [Au<sup>I</sup>(PyBTM)PPh<sub>3</sub>]<sup>+</sup>BF<sub>4</sub><sup>-</sup> (1BF<sub>4</sub>) was also prepared by a slightly modified method and used for optical measurements: the perchlorate salts are generally avoided because they are potentially explosive. No clear

[\*] Y. Hattori, Dr. T. Kusamoto, Prof. Dr. H. Nishihara  
 Department of Chemistry, School of Science  
 The University of Tokyo  
 7-3-1 Hongo, Bunkyo-ku, Tokyo, 113-0033 (Japan)  
 E-mail: kusamoto@chem.s.u-tokyo.ac.jp  
 nisihara@chem.s.u-tokyo.ac.jp  
 Homepage: [http://www.chem.s.u-tokyo.ac.jp/users/inorg/new\\_en/index.html](http://www.chem.s.u-tokyo.ac.jp/users/inorg/new_en/index.html)

[\*\*] We are grateful to Dr. Reizo Kato at RIKEN for his kind provision of facilities and laboratory equipment. This work was supported financially by Grants-in-Aid from MEXT of Japan (Grants 26220801, 24750142, and 21108002; area 2107 (coordination programming)), and MERIT (Material Education Program for the future leaders in Research, Industry, and Technology) in the MEXT Leading Graduate School Doctorial Program.

Supporting information for this article is available on the WWW under <http://dx.doi.org/10.1002/anie.201411572>.

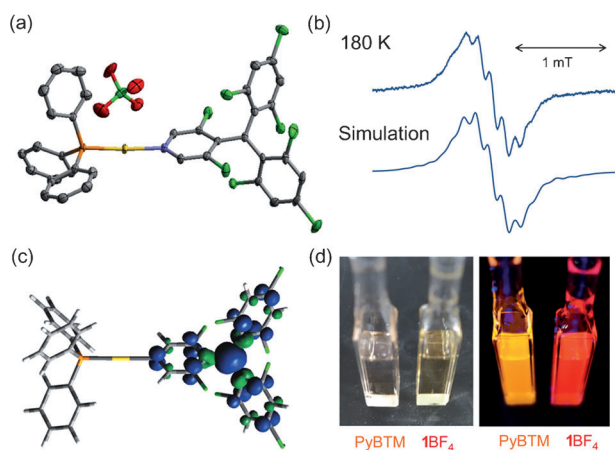


**Figure 2.** a) Crystal structure of  $1\text{ClO}_4$  with ellipsoids set at 50% probability. One cation and one anion for two sets of crystallographically independent molecules are shown. Hydrogen atoms are omitted for clarity. b) ESR spectrum of  $1\text{ClO}_4$  in  $\text{CH}_2\text{Cl}_2$  at 180 K (top) and computer simulation (bottom). c) Calculated spin density distribution of  $1^+$ . d) Photographs of PyBTM and  $1\text{BF}_4$  solutions in dichloromethane under room light (left) and under UV light at  $\lambda = 365$  nm (right).

difference was observed in the optical properties of  $1\text{ClO}_4$  and  $1\text{BF}_4$ .

Single-crystal X-ray diffraction studies revealed the molecular structure of  $1^+$  in the crystalline state (Figure 2a; Supporting Information, Table S1).<sup>[11]</sup> Single crystals of  $1\text{ClO}_4$  contained two sets of crystallographically independent cations and anions. The two cations of  $1$  have similar structures: the N–Au–P angles are both  $176^\circ$  and the perchlorate ions do not coordinate to the  $\text{Au}^1$  center, indicating a two-coordinate linear structure. No intermolecular Au–Au contacts (aurophilic bonds) are observed, probably because of the bulkiness of the triphenylphosphine and PyBTM moieties.

An ESR spectrum in  $\text{CH}_2\text{Cl}_2$  was recorded at 180 K to examine the spin density distribution (Figure 2b). The  $g$  value (2.004) was similar to that of PyBTM. The spectrum showed hyperfine coupling with  $^1\text{H}$ ,  $^{14}\text{N}$ ,  $^{13}\text{C}$ , and  $^{31}\text{P}$  atoms, and was fitted by computer simulation. The obtained hyperfine coupling constants (hccs) were qualitatively similar to those calculated using density functional theory (DFT; Supporting Information, Table S2). The results confirmed that the spin density in  $1^+$  was distributed mainly on the PyBTM ligand (Figure 2c).

MOs of  $1^+$  were calculated using DFT (UM06/SDD(Au), 6-31G(d)(H, C, N, P, Cl)) (Figure 3). The singly occupied molecular orbital of  $1^+$  (SOMO;  $207\alpha$ ) and the lowest-unoccupied spin orbital ( $207\beta$ ) are delocalized mainly on the PyBTM ligand; the electron density distributions are similar to those of PyBTM. The MOs  $206\alpha$ ,  $208\alpha$ ,  $206\beta$ , and  $208\beta$  are all distributed on the PyBTM moiety, with small electron densities on the  $\text{Au}^1$  atom in  $208\alpha$  and  $208\beta$ . Namely, the MOs of  $1^+$  around its frontier orbitals are centered on the PyBTM moiety. These results indicate that the PyBTM moiety plays a main role in the electrochemical and optical properties of the complex.  $\text{PPh}_3$ -centered and  $\text{Au}^1$ -centered orbitals are observed in the lower energy region ( $201\beta$  and  $191\beta$ ; Supporting Information, Figure S1).

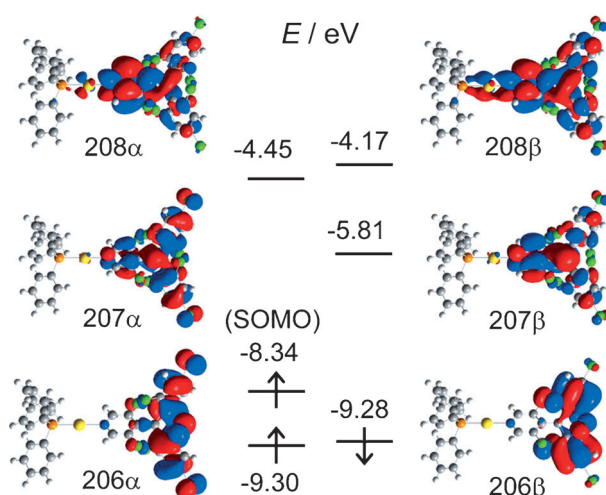


**Figure 3.** Molecular orbitals of  $1^+$  calculated using DFT (UM06/SDD(Au), 6-31G(d)(H, C, N, P, Cl)).

Coordination to  $\text{Au}^1$  lowers the MO energies compared with those of PyBTM. The lower energies of the frontier orbitals (MOs  $207\beta$  and  $207\alpha$ ) were confirmed by the cyclic voltammogram in  $0.1\text{M Bu}_4\text{NClO}_4/\text{CH}_2\text{Cl}_2$  (Supporting Information, Figure S2). The reversible reduction potential attributed to the injection of an electron into  $207\beta$  at  $E^{\text{red}} = -0.21$  V vs. ferrocenium/ferrocene ( $\text{Fc}^+/\text{Fc}$ ) was more positive than that of PyBTM ( $E^{\text{red}} = -0.74$  V). This means that an electron is more easily accepted in  $1^+$  than in PyBTM owing to the electrostatic effect of the cationic  $\text{Ph}_3\text{PAu}^+$  moiety. The irreversible oxidation peak of  $1^+$  ( $E_{\text{p(ox)}} = +1.11$  V), which reflects the energy of  $207\alpha$ , was slightly more positive than that of PyBTM ( $E_{\text{p(ox)}} = +1.04$  V).

$1\text{BF}_4$  displayed three characteristic transition bands at  $\lambda_{\text{abs}} = 566$ ,  $434$ , and  $380$  nm in the UV/Vis absorption spectrum (Figure 4). Each transition was assigned based on the time-dependent (TD)-DFT calculations, which confirmed that the transition processes in the visible region were attributed to the PyBTM ligand (Supporting Information, Figure S3). The excitation of the transition band at the longest wavelength, attributed to the  $206\beta \rightarrow 207\beta$  transition, forms the  $\text{D}_1$  state, from which the fluorescence of  $1\text{BF}_4$  arises. The

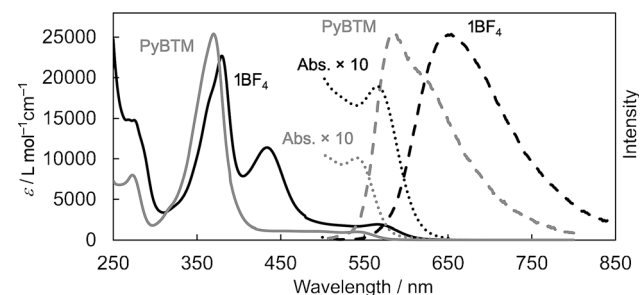


**Figure 4.** Absorption spectra of PyBTM (gray line) and  $1\text{BF}_4$  (black line) and corrected emission spectra of PyBTM (gray dashed line,  $\lambda_{\text{ex}} = 370$  nm) and  $1\text{BF}_4$  (black dashed line,  $\lambda_{\text{ex}} = 435$  nm) in  $\text{CH}_2\text{Cl}_2$ . Enlarged portions of the absorption spectra (ten-fold) are shown from  $\lambda = 500$  to  $650$  nm (gray dotted line for PyBTM and black dotted line for  $1\text{BF}_4$ ).

maximum peak wavelengths of the transition band and the resulting fluorescence band ( $\lambda_{\text{em}} = 653 \text{ nm}$ ) were bathochromically shifted compared with those of PyBTM ( $\lambda_{\text{em}} = 585 \text{ nm}$ ) owing to the lower energy of 207 $\beta$  (Figure 2 d and Figure 4). It should be noted that **1BF**<sub>4</sub> is the first example of a luminescent metal complex that contains a luminescent organic radical as a ligand. This result is in contrast with previously reported Au<sup>I</sup>PPh<sub>3</sub> complexes that exhibit luminescent properties with shorter emission wavelengths.<sup>[9]</sup> The absorption band at 434 nm is assigned as mainly from the 207 $\alpha \rightarrow$ 208 $\alpha$  transition, which corresponds to the transition at 370 nm for PyBTM; the band was also bathochromically shifted. The band at 380 nm probably originates from transitions such as 207 $\alpha \rightarrow$ 213 $\alpha$  and 195 $\beta \rightarrow$ 207 $\beta$ .

The coordination of PyBTM to Au<sup>I</sup> improved the photoluminescence quantum yield in solution. **1BF**<sub>4</sub> in dichloromethane showed an absolute photoluminescence quantum yield ( $\phi$ ) of 8% (Supporting Information, Table S3). The value was four times that of PyBTM ( $\phi = 2\%$ ). The fluorescence lifetime measurements revealed that **1BF**<sub>4</sub> showed a single-component exponential decay with a lifetime  $\tau$  of  $13.1 \pm 0.2 \text{ ns}$ ; this value was about twice that of PyBTM ( $\tau = 6.4 \pm 0.2 \text{ ns}$ ). The prolonged lifetime would contribute to enhancing the luminescence quantum yield.

We estimated the radiative and non-radiative rate constants,  $k_f$  and  $k_{\text{nr}}$ , of **1BF**<sub>4</sub> and PyBTM by using Equations (1)

$$\phi = k_f / (k_f + k_{\text{nr}}) \quad (1)$$

and (2), to reveal the origin of the improvement in the

$$\tau = 1 / (k_f + k_{\text{nr}}) \quad (2)$$

quantum yield (Table 1). The quadrupling of the quantum yield of **1BF**<sub>4</sub> (from 2% to 8%) originated from two factors:

**Table 1:** Photophysical parameters of compounds.

	$\phi$	$\tau$ [ns]	$k_f$ [ $\times 10^6 \text{ s}^{-1}$ ]	$k_{\text{nr}}$ [ $\times 10^6 \text{ s}^{-1}$ ]
PyBTM	0.02	$6.4 \pm 0.2$	3	153
<b>1BF</b> <sub>4</sub>	0.08	$13.1 \pm 0.2$	6	70

the doubling of  $k_f$  and the halving of  $k_{\text{nr}}$ . The increase of  $k_f$  was explained by the greater oscillator strength (absorption coefficient) at the lowest-excited transition (206 $\beta \rightarrow$ 207 $\beta$  transition; Figure 4). This transition corresponds to a forbidden transition for a triarylmethyl radical with an ideal three-fold symmetric structure.<sup>[10]</sup> For PyBTM and **1**<sup>+</sup>, the three-fold symmetries are broken and the transitions are partly allowed. Because of the coordination of PyBTM to the Au<sup>I</sup>PPh<sub>3</sub><sup>+</sup> moiety, the symmetry is lower in **1**<sup>+</sup> than in PyBTM, resulting in the greater absorption coefficient in **1**<sup>+</sup>. The higher oscillator strength in **1**<sup>+</sup> was supported by the TD-DFT calculations.

The decrease of  $k_{\text{nr}}$  might result from suppression of the thermal molecular motion, which is a main factor for non-radiative decay in PyBTM. We propose that the coordination

to Au<sup>I</sup>, a heavy atom, could decrease the thermal fluctuation and vibration of the molecule.

Improvement of photostability is an important issue to be overcome for luminescent radicals. We have reported that the photostability of PyBTM is up to 115 times higher than that of tris(1,3,5-trichlorophenyl)methyl radical, a previously reported luminescent radical. The decay of the fluorescence intensity was investigated for **1BF**<sub>4</sub> in dichloromethane upon irradiation with light at  $\lambda = 370 \text{ nm}$  to elucidate the effect of the coordination to Au<sup>I</sup> on the photostability of the compound. The estimated half-life ( $t_{1/2}$ ) was  $(5.0 \pm 1.1) \times 10^4 \text{ s}$ ; this value was three times larger than that of PyBTM ( $(1.5 \pm 0.2) \times 10^4 \text{ s}$ ) in the same condition, indicating that **1BF**<sub>4</sub> has superior photostability to PyBTM (Figure 5; Supporting Information,

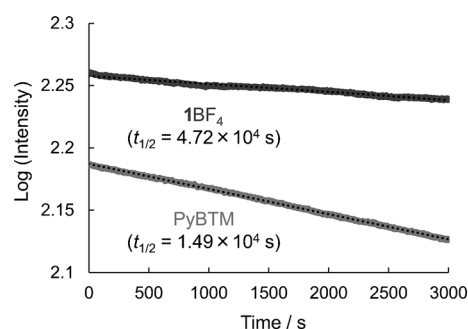


**Figure 5.** Plots showing the emission decay of PyBTM and **1BF**<sub>4</sub> in dichloromethane under continuous excitation with light at  $\lambda_{\text{ex}} = 370 \text{ nm}$ . The half-lives ( $t_{1/2(\text{PyBTM})} = (1.5 \pm 0.2) \times 10^4 \text{ s}$ ,  $t_{1/2(\text{1BF}_4)} = (5.0 \pm 1.1) \times 10^4 \text{ s}$ ) were estimated from repeated experiments (Supporting Information, Figure S4, Table S3).

Figure S4, Table S3). The lower energy levels of the frontier orbitals involved in the photophysical process, as shown by cyclic voltammetry and DFT, contribute to the enhanced photostability.<sup>[5]</sup> The results show that the coordination positively affected the photophysical ( $\phi$ ) and photochemical ( $t_{1/2}$ ) properties.

In conclusion, we prepared the first luminescent metal complex (**1**<sup>+</sup>) with a coordinated luminescent radical. The complex exhibited fluorescence from the D<sub>1</sub> state to the D<sub>0</sub> state transition that was attributed to the PyBTM moiety. The coordination of PyBTM to Au<sup>I</sup> had a positive effect on the photophysical and photochemical properties by increasing the fluorescence wavelength, quantum yield, and photostability.

Received: December 1, 2014

Published online: February 4, 2015

**Keywords:** gold · luminescence · N ligands · photostability · radicals

[1] M. Asano, Y. Kaizu, H. Kobayashi, *J. Chem. Phys.* **1988**, *89*, 6567–6576.

[2] a) K. Ishii, J. Fujisawa, Y. Ohba, S. Yamaguchi, *J. Am. Chem. Soc.* **1996**, *118*, 13079–13080; b) K. Ishii, J. Fujisawa, A. Adachi,

- S. Yamauchi, N. Kobayashi, *J. Am. Chem. Soc.* **1998**, *120*, 3152–3158.
- [3] a) M. V. Encinas, E. A. Lissi, J. Alvarez, *Photochem. Photobiol.* **1994**, *59*, 30–34; b) V. Maurel, M. Laferrière, P. Billone, R. Godin, J. C. Scaiano, *J. Phys. Chem. B* **2006**, *110*, 16353–16358; c) J. Hong, Y. Zhuang, X. Ji, X. Guo, *Analyst* **2011**, *136*, 2464–2470.
- [4] a) V. Gamero, D. Velasco, S. Latorre, F. López-Calahorra, E. Brillas, L. Juliá, *Tetrahedron Lett.* **2006**, *47*, 2305–2309; b) D. Velasco, S. Castellanos, M. López, F. López-Calahorra, E. Brillas, L. Juliá, *J. Org. Chem.* **2007**, *72*, 7523–7532; c) L. Fajalí, R. Papoular, M. Reig, E. Brillas, J. L. Jorda, O. Vallocorba, J. Rius, D. Velasco, L. Juliá, *J. Org. Chem.* **2014**, *79*, 1771–1777; d) A. Heckmann, S. Dümmler, J. Pauli, M. Margraf, J. Köhler, D. Stich, C. Lambert, I. Fischer, U. Resch-Genger, *J. Phys. Chem. C* **2009**, *113*, 20958–20966.
- [5] Y. Hattori, T. Kusamoto, H. Nishihara, *Angew. Chem. Int. Ed.* **2014**, *53*, 11845–11848; *Angew. Chem.* **2014**, *126*, 12039–12042.
- [6] a) A. Company, N. Roques, M. Güell, V. Mugnaini, L. Gómez, I. Imaz, A. Datcu, M. Solà, J. M. Luis, J. Veciana, X. Ribas, M. Costas, *Dalton Trans.* **2008**, 1679–1682; b) A. Datcu, N. Roques, V. Jubera, D. MasPOCH, X. Fontrodona, K. Wurst, I. Imaz, G. Mouchaham, J.-P. Sutter, C. Rovira, J. Veciana, *Chem. Eur. J.* **2012**, *18*, 152–162.
- [7] a) A. Barbieri, G. Accorsi, N. Armaroli, *Chem. Commun.* **2008**, 2185–2193; b) V. W.-W. Yam, V. K. K.-W. Lo, *Chem. Soc. Rev.* **1999**, *28*, 323–334; c) V. W.-W. Yam, E. C.-C. Cheng, *Chem. Soc. Rev.* **2008**, *37*, 1806–1813.
- [8] M. Munakata, S.-G. Yan, M. Maekawa, M. Akiyama, S. Kitagawa, *J. Chem. Soc. Dalton Trans.* **1997**, 4257–4262.
- [9] a) L. A. Mullice, F. L. Thorp-Greenwood, R. H. Laye, M. P. Coogan, B. M. Kariuki, S. J. A. Pope, *Dalton Trans.* **2009**, 6836–6842; b) C.-W. Hsu, C.-C. Lin, M.-W. Chung, Y. Chi, G.-H. Lee, P.-T. Chou, C.-H. Chang, P.-Y. Chen, *J. Am. Chem. Soc.* **2011**, *133*, 12085–12099; c) M. Bardají, A. B. Miguel-Coello, P. Espinet, *Inorg. Chim. Acta* **2012**, *392*, 91–98.
- [10] T. L. Chu, S. I. Weissman, *J. Chem. Phys.* **1954**, *22*, 21–25.
- [11] CCDC-1034361 (IClO<sub>4</sub>) contains the supplementary crystallographic data for this paper. The data can be obtained free of charge from The Cambridge Crystallographic Data Centre via [www.ccdc.cam.ac.uk/data\\_request/cif](http://www.ccdc.cam.ac.uk/data_request/cif).